NeuroImage 140 (2016) 110–117

Contents lists available at ScienceDirect

NeuroImage

journal homepage: www.elsevier.com/locate/ynimg

Transcranial electrical stimulation of the occipital cortex during visual perception modifies the magnitude of BOLD activity: A combined tES–fMRI approach

Ivan Alekseichuk [a,*], Kersten Diers [b], Walter Paulus [a], Andrea Antal [a]

[a] Department of Clinical Neurophysiology, University Medical Center Göttingen, Georg-August University Göttingen, 37075 Göttingen, Germany
[b] Department of Psychology, Dresden University of Technology, 01062 Dresden, Germany

ARTICLE INFO

Article history:
Accepted 13 November 2015
Available online 23 November 2015

Keywords:
tDCS
tACS
fMRI
Occipital cortex
Visual perception

ABSTRACT

The aim of this study was to investigate if the blood oxygenation level-dependent (BOLD) changes in the visual cortex can be used as biomarkers reflecting the online and offline effects of transcranial electrical stimulation (tES). Anodal transcranial direct current stimulation (tDCS) and 10 Hz transcranial alternating current stimulation (tACS) were applied for 10 min duration over the occipital cortex of healthy adults during the presentation of different visual stimuli, using a crossover, double-blinded design. Control experiments were also performed, in which sham stimulation as well as another electrode montage were used. Anodal tDCS over the visual cortex induced a small but significant further increase in BOLD response evoked by a visual stimulus; however, no aftereffect was observed. Ten hertz of tACS did not result in an online effect, but in a widespread offline BOLD decrease over the occipital, temporal, and frontal areas. These findings demonstrate that tES during visual perception affects the neuronal metabolism, which can be detected with functional magnetic resonance imaging (fMRI).

Introduction

During the last decade, two methods dominated the field of non-invasive electrical stimulation (tES) of the human brain: transcranial direct current (tDCS) and, increasingly, alternating current stimulation (tACS). Animal studies demonstrated that tDCS can modify the membrane potential of neurons and modulate spontaneous firing rates: cathodal stimulation hyperpolarizes, while anodal stimulation depolarizes the resting membrane potential (Bindman et al., 1964; Creutzfeldt et al., 1962; Ranieri et al., 2012). In the current literature, stimulation is defined as cathodal or anodal for a given area depending on the spatial proximity of that anatomical location to the corresponding electrode. During tACS, the externally applied alternating current is assumed to entrain endogenous neural oscillations possibly by increasing the power of oscillations or the phase synchronization between the driving and the endogenous oscillations (Ali et al., 2013; Antal et al., 2008; Cecere et al., 2015; Helfrich et al., 2014; Neuling et al., 2013).

Roughly, 90% of the conceptional framework of manipulating cortical excitability in human subjects by transcranial stimulation techniques has been obtained at the motor cortex (M1) (for a review, see Nitsche and Paulus, 2011). This is due to the comparatively easy acquisition and analysis of the transcranial magnetic stimulation (TMS)-induced motor-evoked potentials (MEPs), which amplitudes presumably reflect the excitability changes of the M1 (Nitsche and Paulus, 2000, 2001). With regard to other cortical areas, different biomarkers can be used, e.g., phosphene threshold measurements during the visual cortex stimulation (Antal et al., 2003a, 2003b) or complex behavioural changes like memory accuracy (Pisoni et al., 2015) or reaction time (Nelson et al., 2014). At present, functional magnetic resonance imaging (fMRI) seems to be the most suitable method having a clear potential to investigate the online effect of the transcranial electrical stimulation techniques with a high spatial resolution (regarding the combination of tES with other methods, see Miniussi et al., 2012; Stagg, 2014). The novel concurrent combination of electrical stimulation and fMRI allows tracing of alterations not only at the stimulation site but also at a remote projection areas within the whole brain, during ongoing or immediately after stimulation (Turi et al., 2012). However, the number of studies using concurrent application of tDCS and fMRI is limited. Interestingly, many of them did not replicate the bipolar effect of tDCS that can be observed in the neurophysiological studies, e.g., after M1 stimulation (Amadi et al., 2014; Antal et al., 2011). The direction and the magnitude of the induced effects also demonstrated high task dependency. For example, it was found that in rest neither anodal nor cathodal tDCS over the M1 induced a detectable BOLD signal change, while anodal stimulation decreased BOLD in the supplementary motor area only during voluntary finger tapping (Antal et al., 2011). In another study, anodal tDCS over the left frontal area facilitated picture

* Corresponding author at: Department of Clinical Neurophysiology, University Medical Center Göttingen, Georg-August University Göttingen, Robert-Koch-Str. 40, 37075, Göttingen, Germany.
E-mail address: ivan.alekseichuk@med.uni-goettingen.de (I. Alekseichuk).

http://dx.doi.org/10.1016/j.neuroimage.2015.11.034
1053-8119/

naming, which was correlated with decreased BOLD response in the Broca's area (Holland et al., 2011). tACS has not been systematically investigated using the functional magnetic resonance imaging yet.

Another functional approach – magnetoencephalography (MEG) – currently is developing as a method that can be combined with tES. First proof-of-concept studies show the possibility to recover the brain oscillations using MEG during the application of tDCS (Garcia-Cossio et al., 2016; Soekadar et al., 2013) as well as tACS (Witkowski et al., 2016) over the motor cortex. While this research strategy was introduced very recently, it is demonstrating a potential to provide a precise mapping of oscillatory entrainment in the neocortex that will complement the future tES studies.

The number of brain stimulation studies targeting the visual cortex is relatively low and the question is still unanswered, if the tES results observed during M1 stimulation can directly be translated to the visual cortex stimulation. The visual and motor cortices vary with regard to the different cytoarchitecture of the cortices and different spatial orientations of the neurons, factors influencing excitatory/inhibitory circuitries. Furthermore, differences in cortical connections and neuronal membrane properties, including receptor expression, may also account for the altered responses. Already early animal experiments demonstrated that the DC effect on the visual cortex was less pronounced than on the M1 (Creutzfeldt et al., 1962). Later human studies confirmed these results (Antal et al., 2001, 2004; Kraft et al., 2010; Olma et al., 2011), demonstrating that the tDCS aftereffects are relatively short lasting in the visual areas compared to those of the M1, using the same stimulation intensity and durations. With regard to tACS, it was suggested that the aftereffect might be longer. Recent tACS-EEG study showed that continuous stimulation in alpha range over the occipital cortex lead to the enhancement of the oscillatory activity during as well as after the stimulation, up to 30 min (Helfrich et al., 2014).

As it was mentioned above, most of the imaging studies have investigated online changes in the motor or prefrontal cortices (for a review, see Saiote et al., 2013). Research with regard to other cortical areas is rather underrepresented. Therefore, our aim was to observe the tES-induced metabolic changes measured by blood oxygen level-dependent (BOLD) activity targeting the visual cortex. We (i) investigated the feasibility of BOLD imaging to detect the effects of tES on the occipital area and (ii) made an attempt to clarify the spatial-temporal organization of the detectable effects.

Materials and Methods

Participants

Sixteen healthy adult volunteers initially signed up for this study. One volunteer was excluded due to non-appearance; thus, 7 males (24.6 ± 1.6 years old) and 8 females (25.1 ± 3.9 years old) took part in the experiment. All participants were interviewed about their state of health: none of them had any neurological or psychiatric disorders, metallic or electric implants, or took any medication during the 4 weeks prior the experimental sessions. They received complete information regarding the exclusion criteria's and possible side effects for tES and MRI and gave their written informed consent to participate according to the regulation of the University Medical Center Goettingen and Declaration of Helsinki. We confirm that the ethical committee of the University of Goettingen approved this study.

Visual stimuli

Visual stimuli were generated using the software package "Presentation" (Neurobehavioral Systems, USA) and were delivered through the MR-suited LCD glasses covering a visual field of 30° in the horizontal and 20° in the vertical direction. We have used two separate visual perception conditions: rotated wedges and expending rings (Fig. 1).

In both cases, volunteers were instructed to focus their attention on the fixation cross in the center of their visual field. No other instructions except of a passive perception were given. During the 6 min achromatic, dartboard contrast pattern (~90% contrast) was presented in the certain area of the screen. The wedge was span 45° of angle and extends to 20° from fixation; it changed the position in the clockwise manner. The ring occupied from 1° to 20° of the visual field in eight subsequent steps. The color of the stimulus was inversed with rate 15 Hz. The position of the stimulus on the screen was changing in every 10 s in synchrony with the MRI data acquisition rate. These stimuli induced BOLD activity that is specific for the processing of the visual information in the left or right side of the visual field and in the center or on the periphery of the visual field (DeYoe et al., 1996; Wandell, Dumoulin, Brewer, 2007; see Supplementary Figs. 1 and 2 for details).

Transcranial direct current and alternating current stimulation (tDCS and tACS)

Stimulation was delivered by the MR-compatible battery-driven stimulator (NeuroConn GmbH, Germany) that was placed outside of the shielded room and connected to the two 5 × 5 cm^2 MR-compatible rubber electrodes through the isolated optical cable with filtering system. The signal-to-noise ratio of the acquired MR images was unaffected by the onset of the electrical stimulation and nonsignificantly decreased (no more than 9%) due to the hardware set up in comparison to the empty room. Electrodes were fixed on the scalp of the participant with conductive paste. We used the following electrode montage: anode over the Oz and cathode over the Cz according to the international 10–20 EEG system. According to the computational model, this placement led to the predominant bihemispheric occipital stimulation with peak field intensity of 0.3 V/m (Supplementary Fig. 3). Calculations were made with the specialized modeling software package "HD-Explore" (Soterix Medical Inc., USA). Stimulation was applied with the intensity of 1 mA peak-to-baseline and duration of 10 min (including 15 s of the fade-in/fade-out periods). This ensured the comparable amount of the ejected energy for the tDCS and tACS, while peak-to-peak amplitude of the alternating current was twice higher than for the direct current due to the existence of the positive and negative phases. In case of tACS, the frequency of the alternating current was 10 Hz. This stimulation frequency lies in the center of the alpha range, which is the dominant oscillatory activity in the human occipital cortex. During the sham control session, the stimulation was limited to the duration of 30 s. Impedance always was kept below 20 kOhm. Additionally, for the control session, we used an additional AC stimulation montage with electrode positions at C5–C6, which focuses the electrical field in the central–frontal region. Each stimulation session was separated from the previous one by at least 48 h.

Functional magnetic resonance imaging (fMRI)

MRI studies were performed at 3 T (Siemens Magnetom Tim Trio, Erlangen, Germany) using a standard 8-channel phased-array head coil. Participants were placed supine inside the magnet bore and wore the headphones for noise protection and MR-suited LCD glasses. Physical and emotional condition of the volunteers was monitored throughout the experiment. At the beginning of every session, we recorded T1-weighted anatomical image with 3D turbo FLASH MRI sequence at 1 mm^3 isotropic resolution (repetition time (TR) = 2250 ms, echo time (TE) = 3.26 ms, inversion time (TI) = 900 ms, flip angle = 9°). For BOLD fMRI a T2*-sensitive gradient-echo echo-planar imaging technique (TR = 2000 ms, TE = 36 ms, flip angle = 70°) at 2 × 2 mm^2 resolution was used. Twenty-eight consecutive sections at 2 mm thickness roughly parallel to the calcarine fissure were acquired, covering the brain areas of interest. Region of interest included the occipital, temporal, frontal, and posterior part of the parietal cortex.

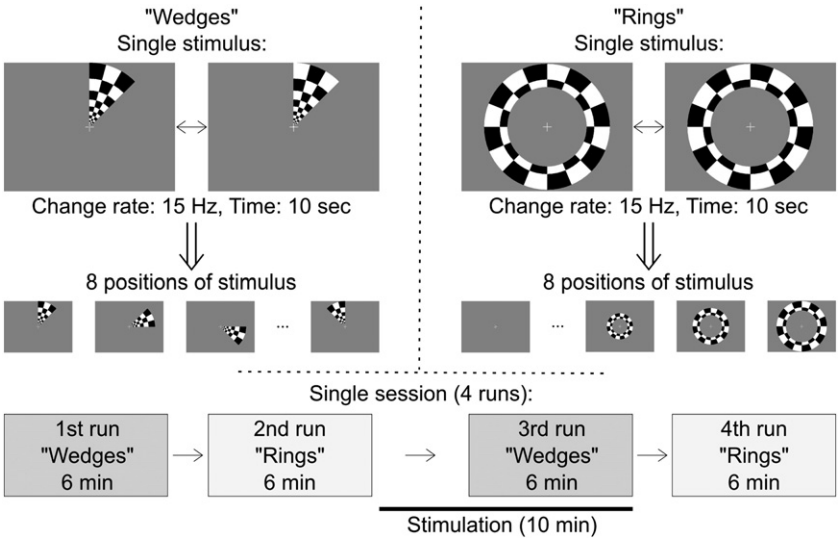

Fig. 1. Visual perception conditions: achromatic, dartboard contrast pattern was presenting in form of the wedge or ring for 10 s per position. In total, there were 8 different positions that were repeated 4 times per run. Lower panel: structure of the single experimental session.

A total of 175 volume images (5 dummy scans, 160 volumes of interest, and 10 blank scans at the end) were acquired during the every run.

Experimental procedure

All participants took part in 4 sessions in randomized order. Each session had the same structure (Fig. 1) with one variable parameter: subjects received (1) DC stimulation over the occipital cortex, (2) AC stimulation over the occipital cortex, (3) sham stimulation over the occipital cortex, or (4) AC stimulation over the central–frontal region. Participants and MRI technician were blinded regarding the type of the stimulation. Every session began with an anatomical scan followed by the 4 runs of data acquisition with 2 min breaks in between the runs. During these breaks, the volunteers received a verbal reminder of the instructions. At the first run, we collected the fMRI data that characterize the visual stimuli "wedges." The second run corresponded to the stimuli "rings." The first and the second runs served as a baseline conditions for evaluation of the current-induced changes in the task-related BOLD activity. Third and fourth runs replicated the visual stimuli during (for the "wedges") and immediately after (for the "rings") the electrical stimulation, respectively. Later on, online effect of the electrical stimulation was described as difference between the BOLD activity at the 3rd and the 1st runs (visual stimuli "Wedges"), and immediate after effect – as difference between the 4th and the 2nd runs (visual stimuli "Rings"). Then the magnitude of the current-induced effects during the DC- and AC-related sessions was compared with the corresponding changes during the sham stimulation.

Data analysis

The fMRI data were processed using Statistical Parametric Mapping software (SPM12; Wellcome Trust Centre for Neuroimaging, UK) running under Matlab 2015a (MathWorks, USA). The first five volumes from every run were discarded to ensure the MRI steady state. Then we performed the temporal correction of the acquired slices within each volume, using the first image as reference. Subject-specific volumes of interest from each experiment were spatially realigned and registered to the mean image. The realignment parameters were saved to account for the residual head-motion effects on the level of the statistical model. Finally, the functional images were coregistered to the individual anatomy, normalized to the standard MNI space and smoothed with an 8 mm full-width at half-maximum isotropic Gaussian kernel. All interpolations were made with the 4th-degree B-spline method.

We computed the statistical model separately for AC and DC stimulations, and for the online effect and aftereffect. On the first level of the analysis, each design matrix included four sessions (stimuli-specific baseline and active run for the real and sham electrical stimulation). Within each session, eight positions of the visual stimulus were included as conditions and described by the boxcar function with duration of 10 s and off period of 70 s. Motion parameters were included as additional regression factors. To remove low frequency drifts, the data were high-pass filtered using a cutoff period of 128 s. Later each condition was modeled by convolving it with the canonical hemodynamic response function. We accounted for the serial correlation using the first order autoregressive function.

In order to estimate the statistical contrasts, all visual stimuli were grouped in four categories depending on their position on the screen and, subsequently, on the visual field: right wedges or left wedges, and central rings or peripheral rings. Contrasts of interest were first defined as the activity during the presentation of a given group of stimuli versus the global activity. Then contrasts related to the electrical stimulation were compared with the corresponding current-free baseline images (stimulation minus baseline). Finally, the stimulation effect was compared with the BOLD alterations during the sham session (baseline-adjusted stimulation session minus baseline-adjusted sham session). On the second level of the statistical analysis, group-averaged parametric maps of the current-induced effect were calculated. For that, a one-sample *T*-test was used. Additionally, the statistical interaction between the electrical stimulation and the position of the visual stimulus on the screen was estimated with an *F*-test. All statistical tests were conducted voxelwise with a significance level $p = 0.001$, uncorrected. Subsequently, cluster size threshold (≥40) was applied to decrease the probability of the false positive findings.

Results

rAll of the subjects tolerated the experimental procedure very well; none of them reported any side effects during or after the stimulation. Two volunteers indicated non-disturbing phosphenes at least once during the measurements with an average magnitude of 3.8 out of 10. The corresponding data sets were not excluded.

Functional MR images were analyzed with focus on the current-specific activity, while the BOLD response on the visual stimuli *per se*

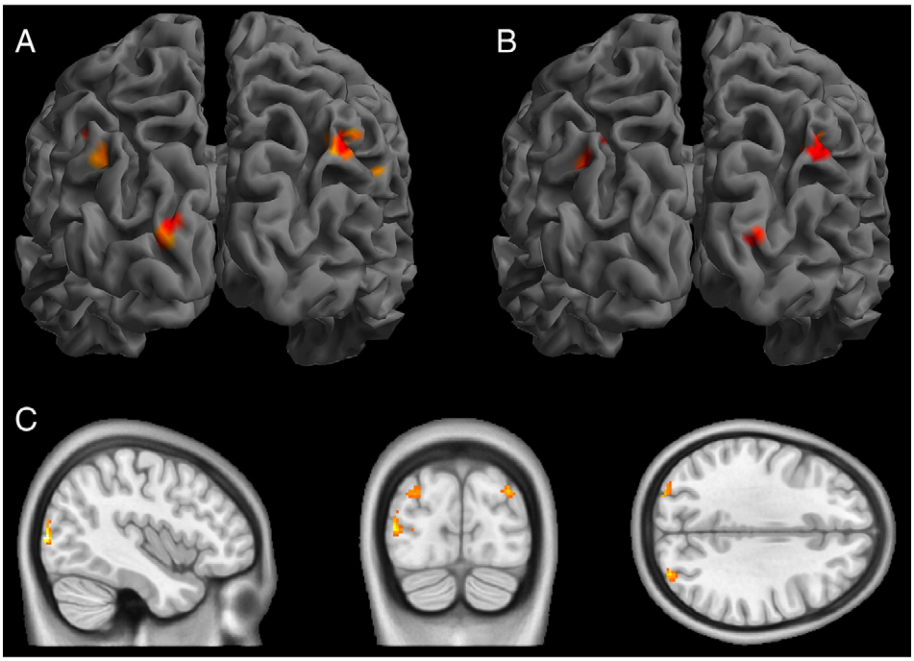

Fig. 2. tDCS-induced modulation of the stimuli-related BOLD activity. Red color indicates lower critical values and yellow indicates higher critical values. Upper panel: clusters of the increased BOLD signal during tDCS and visual stimulation in the right (A) or left (B) field of view. Lower panel (C): clusters of the statistical interaction between the DC stimulation and the visual stimulus. See corresponding Table 1 (section 1) for the details.

was considered being a baseline. Given that two different visual stimuli were used to evaluate the online and aftereffect of the stimulation, the corresponding global BOLD activity during the baseline run "rings" and the baseline run "wedges" were compared across all sessions. No statistical difference ($p < 0.001$, cluster size ≥40) was observed.

Transcranial direct current stimulation (tDCS) and sham stimulation

An increase in the BOLD signal during the anodal DC stimulation in comparison to the current-free baseline run was observed ($p < 0.001$, cluster size ≥40). The significant changes were localized in the occipital–parietal area (Figs. 2A, B and Table 1, section 1).

Table 1
DC-induced activation locations. Critical values correspond to the one-sample *T*-test or *F*-test ($n = 15$, $p < 0.001$, cluster size ≥40). Coordinates of the voxel with maximum critical value are given in MNI space.

Anatomical region	Side	Coordinates (*x*/*y*/*z*)	Critical value, ±*T*(14)	Cluster size
1. Online effect of the anodal tDCS over the occipital cortex (see Fig. 2)				
Visual stimulus in the right field of view				
Cuneus	L	−14/−96/18	+4.86	65
Angular gyrus	L	−38/−66/40	+5.17	82
Middle occipital and angular gyrus	R	48/−68/40	+5.23	89
Precuneus	R/L	2/−68/28	+4.02	97
Visual stimulus in the left field of view				
Cuneus	R	20/−98/12	+4.32	42
Middle occipital and angular gyrus	R	46/−72/38	+4.71	67
Middle occipital and angular gyrus	L	−32/−70/36	+4.33	55
Statistical interaction between the visual stimulus and tDCS			*F*(1,14)	
Middle occipital gyrus	R	32/−84/32	24.60	48
Middle occipital gyrus	L	−30/90/30	22.34	44
Inferior occipital gyrus	L	−42/−88/6	29.17	90
2. Online effect of the sham stimulation				
No suprathreshold clusters				
3. Online effect of the anodal tDCS over the occipital cortex minus effect of the sham stimulation				
Visual stimulus in the right field of view				
Middle occipital gyrus	R	26/−92/4	+4.27	70
Superior occipital gyrus	L	−16/−96/18	+4.31	73
Calcarine	R	18/−100/−6	+4.55	93
Visual stimulus in the left field of view				
Middle occipital gyrus	L	−32/−72/34	+4.49	89
Middle occipital gyrus	R	40/−70/34	+4.43	167
Cuneus	R/L	0/−78/28	+4.09	42

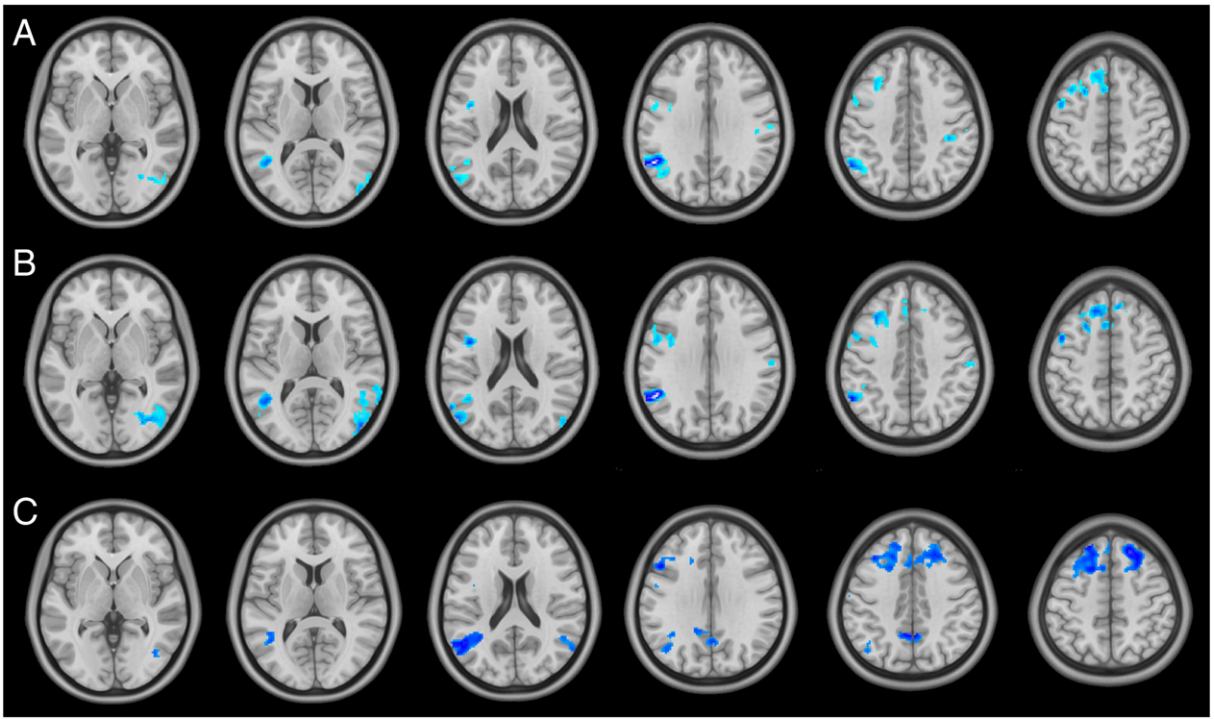

Fig. 3. AC-induced modulation of the stimuli-related BOLD activity. Brain slices are given in the axial plane with coordinates from 0 to 60 mm in MNI space. Light blue color indicates lower critical values and dark blue indicates higher critical values. Panel A: clusters of the decreased BOLD signal after the tACS over the occipital cortex associated with the visual stimulus in the center of the field of view. Panel B: clusters of the decreased BOLD signal after the tACS over the occipital cortex associated with the visual stimulus on the periphery of the field of view. See corresponding Table 2 (section 1) for the details. Panel C: BOLD activity after tACS over the occipital region minus BOLD activity after tACS over the central–frontal region.

The spatial distribution of the effect was in agreement with the expected route of the current flow (bihemispheric occipital–parietal regions, see Supplementary Fig. 3 for details) and demonstrated stimulus specificity: further increase in the activity in the occipital pole was linked to the presentation of the visual stimulus in the opposite hemisphere of the field of view. The statistical interaction between the electrical stimulation and the position of the visual stimulus was located in the visual cortex as well (Fig. 2C). At the same time, sham stimulation did not induce any detectable alterations in the BOLD response. Subsequent statistical comparison of the effect of the anodal tDCS with the effect of the sham stimulation confirmed the occipital localization of the current-induced changes (Table 1, section 3). Concerning the aftereffect of the stimulation, there was no significant current-specific BOLD alterations.

Transcranial alternation current stimulation (tACS)

Transcranial AC current, on the contrary, did not lead to a significant online cortical effect when the stimulation was applied either over the occipital cortex or over the central–frontal region. Nevertheless, evaluation of the immediate afteraffect revealed prominent decrease of the BOLD signal (Fig. 3 and Table 2). With regard to the occipital cortex stimulation, this decrease occurred both in visual-related areas (inferior and middle occipital gyrus) and in distant regions (Table 1, section 1), while AC stimulation over the central–frontal cortex did not induce any effect in the occipital area (Table 1, section 2). Comparison of the aftereffect of tACS over the occipital cortex and the aftereffect of the sham stimulation (Table 2, section 3) confirmed the direction and spatial localization of the current-induced BOLD modification: a decrease of the signal was detected in the occipital as well as the parietal–frontal region.

Discussion

In this study, we have demonstrated that tES applied over the occipital cortex during visual perception affects the neuronal metabolism, which can be detected by changes in the BOLD fMRI. However, the induced BOLD activity modifications were highly dependent on the type of the stimulation: regarding tDCS, the online effect of the anodal stimulation was small; however, the observed increase in the BOLD signal was mostly localized in the visual cortex or functionally related areas to the maximum electrical field. Based on the dominant theory of the tDCS mechanism (Bindman et al., 1964; Rahman et al., 2013), which suggests that DC is shifting the membrane potential of the neuronal cells that are orthogonal to the electrical current, we hypothesized that the effect of the anodal stimulation would accumulate over time, resulting in more prominent changes. In opposite to our expectation, the aftereffect of the stimulation in the current study was not significant on the level of BOLD response.

Nevertheless, so far there are not enough experimental data in order to make a solid speculation regarding the relationships between the effect of the electrical field, the localization of the physiological effect, and the appearance of the BOLD response change in the brain. However, it is already clear that these three factors probably do not have linear and trivial dependencies. With regard to the basic mechanisms of the BOLD fMRI, contradictory to the intuitive expectations, increase or decrease of the BOLD signal is predominantly corresponding to the changes in excitation–inhibition balance in the neuronal microcircuits rather than to the local neuronal spiking rate alteration (Logothetis, 2008). Thus, absence of the significant BOLD response in the target area should not be treated as the complete absence of the effect.

Previous neurophysiological studies have shown that anodal tDCS is also able to modulate the activity of the visual cortex, by decreasing phosphene thresholds (Antal et al., 2003a, 2003b), improving contrast perception (Kraft et al., 2010) and increasing the amplitude of visual-evoked potentials (Antal et al., 2004). According to these results, our BOLD increase during anodal stimulation might represent an improvement in visual perception. Nevertheless, in our present study the observed BOLD change is minor, suggesting that anodal stimulation might have a ceiling effect here. Furthermore, the relationship between

Table 2
AC-induced activation locations. Critical values correspond to the one-sample *T*-test ($n = 15$, $p < 0.001$, cluster size ≥40). Coordinates of the voxel with maximum critical value are given in MNI space.

Anatomical region	Side	Coordinates (*x*/*y*/*z*)	Critical value, ±*T*(14)	Cluster size
1. Aftereffect of the tACS over the occipital cortex (see Figs. 3A, B)				
Visual stimulus in the center of the field of view				
Inferior occipital gyrus	R	40/−74/−2	−6.03	237
Middle occipital, angular, inferior parietal, middle temporal and supramarginal gyrus	L	−54/−54/30	−8.56	965
Precentral and middle frontal gyrus	L	−46/4/46	−5.96	589
Supramarginal gyrus	R	60/−22/34	−5.26	183
Superior frontal gyrus and supplementary motor area	L	−8/24/46	−4.56	228
Visual stimulus on the periphery of the field of view				
Middle occipital, inferior occipital and middle temporal gyrus	R	46/−80/10	−5.74	767
Middle occipital, angular, supramarginal and middle temporal gyrus	L	−52/−52/30	−7.91	966
Medial superior frontal gyrus	R	12/30/44	−6.32	124
Middle frontal and precentral gyrus	L	−46/4/46	−6.60	676
Superior frontal gyrus	L	−4/34/46	−5.54	612
Postcentral gyrus	R	60/−20/34	−4.08	113
2. Aftereffect of the tACS over the central–frontal cortex				
Visual stimulus in the center of the field of view				
Superior frontal and middle frontal gyrus	R	22/34/48	+4.93	427
Superior frontal gyrus	L	−12/20/48	+4.55	114
Middle temporal gyrus	L	−50/−68/6	−7.67	142
Visual stimulus on the periphery of the field of view				
Superior frontal and middle frontal gyrus	R	22/32/48	+4.59	373
Superior frontal and middle frontal gyrus	L	−14/20/48	+4.33	211
Middle temporal gyrus	L	−52/−72/4	−4.38	67
3. Aftereffect of the tACS over the occipital cortex minus aftereffect of the sham stimulation				
Visual stimulus in the center of the field of view				
Inferior occipital gyrus	R	40/−72/−4	−4.49	84
Superior and middle occipital gyrus	R	24/−76/18	−4.35	73
Middle temporal gyrus	R	60/−64/2	−4.58	250
Middle temporal gyrus	L	−62/−48/0	−4.16	72
Precentral gyrus	R	54/4/30	−4.21	88
Visual stimulus on the periphery of the field of view				
Middle occipital and middle temporal gyrus	L	−54/−70/12	−5.02	278
Inferior occipital gyrus	R	36/−70/6	−4.06	76
Lingual gyrus	L	−18/−74/−6	4.13	83
Middle temporal gyrus	R	60/−64/2	−4.63	223
Precentral gyrus	R	56/8/34	−4.88	115

tDCS-induced neurophysiological and BOLD changes might not be straightforward and linear, and electrode positions should be taken into account. For example, it is well known that anodal tDCS over the M1 increases MEP size in rest and decreases them when coexist with motor movement (Antal et al., 2007). However, during the finger tapping, it resulted in a decrease in the BOLD response, not in the M1 but in the SMA (Antal et al., 2011). In another study, anodal stimulation during learning of a visuomotor task did not result in significant performance or BOLD changes compared to the placebo stimulation (Saiote et al., 2013). Concerning other stimulation sites, it was demonstrated that anodal tDCS over the left frontal cortex increases the reaction time in a naming task and decreases BOLD activity in the Broca area (Holland et al., 2011), and it improves the performance of older adults in semantic word generation task by affecting the related resting state fMRI connectivity (Meinzer et al., 2013). Taken together, most results suggest a reduction of the BOLD response by anodal tDCS, opposite to the increase seen here. It seems to be that direction of the effect depends on the nature and state of the target brain area.

The magnitude of the small anodal effect can also be explained by the low stimulation intensity. The occipital bones are thicker than the bones over the frontal areas, thus the distance between the stimulating electrode and the targeted cortical area is longer in case of the visual cortex, compared to M1 stimulation. Therefore, it is possible that in case of the visual cortex stimulation, higher intensities would change the BOLD response more effectively. The cytological organization and functional dynamics of the occipital cortex are substantially different compared to the motor cortex, which can also lead to the less stable effect of the membrane hypo- or depolarization. Interestingly, the increase in the BOLD activity after tDCS with intensity of 1 mA was previously demonstrated for the cathodal stimulation of the motion sensitive area V5 (Antal et al., 2012). This difference may come from observations that anodal and cathodal stimulation induces different changes of GABA level (Stagg et al., 2009). The absence of the detected aftereffect for tDCS in the current study can also be explained by the data of a previous study: by measuring the amplitude of the visual-evoked potentials, it was demonstrated that anodal polarization decayed after 4 min post-stimulation (Accornero et al., 2007).

Previous studies found that natural alpha power increase is associated with inhibition in the firing rates, reduced phosphene detection, and smaller BOLD signal (Haegens et al., 2011; Ritter et al., 2009; Romei et al., 2008). Therefore, we anticipated that our transcranial 10 Hz stimulation might also decrease the BOLD response. However, in case of tACS, our primary finding is the absence of meaningful significant BOLD activity change during the stimulation, but strong, widely spread decrease of the signal immediately after the stimulation. These results are in line with the commonly accepted hypothesis that tACS relies on the effects of the functional resonance between the applied field and the local oscillatory activity (Ali et al., 2013; Fröhlich and McCormick,

2010) and, subsequently, on the modulation of the short- and long-range connectivity by the phase shift rather than on the "mechanical" modulation of the neuronal excitability like in case of tDCS. Again, we can only speculate that the lack of an online effect of tACS over the targeted area may be due to the insufficient time or intensity of the stimulation. Reports in the literature regarding the minimal sufficient intensity of the applied electrical current in order to induce an effect are contradictory and vary between 0.2 and 0.5 V/m (Herrmann et al., 2013; Reato et al., 2010). The other possibility is that 10 Hz tACS-induced entrainment that can be observed in previous neurophysiological studies (e.g., Zaehle et al., 2010) does not induce an extra cost in the metabolism or the changes is too small to cause a BOLD alterations. The principal difference in the mechanisms of the DC and AC stimulation can drive the fact that the stimulation with close to the border intensity leads to the predominant effect during or immediately after the stimulation, respectively.

The AC stimulation over the central–frontal cortex did not lead to an online effect as well but caused both increase and decrease of the BOLD signal in the parietal–frontal regions after stimulation. The lack of significant changes in the occipital area is supporting the task relevance of the AC stimulation.

With regard to the limitations of this study, it remains unclear whether the implementation of other parameters and montages, e.g., the multi-electrode array with the individually pre-define montage and intensity, or individualized AC frequencies, could have a significant impact on BOLD activity change. Additionally, it should be noted that due to the absence of a cognitive task or a technical device (e.g., eye tracking) that could ensure focusing the volunteer's attention, the results of this study may be diluted with a non-specific effects. Post hoc screening, however, suggests that the volunteers carefully followed the instructions.

Taking together, our results indicate that both DC and AC current affect the neuronal activity in the occipital cortex, which can be observed by BOLD fMRI. While tDCS over the occipital cortex during visual perception led to small, transient, but significant increase in the BOLD activity in the stimulated area, tACS with frequency of 10 Hz provokes a widely spread decrease of the BOLD signal immediately after the stimulation. Further implementation of the concurrent fMRI-tES with more complicated paradigms, including research of the complex cognitive functions and state-dependent connectivity, should be accompany with careful planning of the stimulation control conditions and cautious interpretation of the findings.

Supplementary data to this article can be found online at http://dx.doi.org/10.1016/j.neuroimage.2015.11.034.

Acknowledgments

This study was supported by the DFG (PA 419/15-1) awarded to WP.

References

Accornero, N., Li Voti, P., La Riccia, M., Gregori, B., 2007. Visual evoked potentials modulation during direct current cortical polarization. Exp. Brain Res. 178 (2), 261–266 (PMID: 17051377).

Ali, M.M., Sellers, K.K., Frohlich, F., 2013. Transcranial alternating current stimulation modulates large-scale cortical network activity by network resonance. J. Neurosci. 33 (27), 11262–11275. http://dx.doi.org/10.1523/JNEUROSCI.5867-12.2013.

Amadi, U., Ilie, A., Johansen-Berg, H., Stagg, C.J., 2014. Polarity-specific effects of motor transcranial direct current stimulation on fMRI resting state networks. NeuroImage 88 (100), 155–161. http://dx.doi.org/10.1016/j.neuroimage.2013.11.037.

Antal, A., Nitsche, M.A., Paulus, W., 2001. External modulation of visual perception in humans. Neuroreport 12 (16), 3553–3555.

Antal, A., Tamas, Z.K., Nitsche, M., Paulus, W., 2003a. Modulation of moving phosphene thresholds by transcranial direct current stimulation of V1 in human. Neuropsychologia 41 (13), 1802–1807. http://dx.doi.org/10.1016/S0028-3932(03)00181-7.

Antal, A., Kincses, T.Z., Nitsche, M., Paulus, W., 2003b. Manipulation of phosphene thresholds by transcranial direct current stimulation in man. Exp. Brain Res. 150 (3), 375–378. http://dx.doi.org/10.1007/s00221-003-1459-8.

Antal, A., Kincses, T.Z., Nitsche, M.A., Bartfai, O., Paulus, W., 2004. Excitability changes induced in the human primary visual cortex by transcranial direct current stimulation: direct electrophysiological evidence. Invest. Ophthalmol. Vis. Sci. 45 (2), 702–707.

Antal, A., Terney, D., Poreisz, C., Paulus, W., 2007. Towards unravelling task-related modulations of neuroplastic changes induced in the human motor cortex. Eur. J. Neurosci. 26, 2687–2691. http://dx.doi.org/10.1111/j.1460-9568.2007.05896.x.

Antal, A., Boros, K., Poreisz, C., Chaieb, L., Terney, D., Paulus, W., 2008. Comparatively weak after-effects of transcranial alternating current stimulation (tACS) on cortical excitability in humans. Brain Stimul. 1 (2), 97–105. http://dx.doi.org/10.1016/j.brs.2007.10.001.

Antal, A., Polania, R., Schmidt-Samoa, C., Dechent, P., Paulus, W., 2011. Transcranial direct current stimulation over the primary motor cortex during fMRI. NeuroImage 55 (2), 590–596. http://dx.doi.org/10.1016/j.neuroimage.2010.11.085.

Antal, A., Kovacs, G., Chaieb, L., Cziraki, C., Paulus, W., Greenlee, M.W., 2012. Cathodal stimulation of human MT+ leads to elevated fMRI signal: a tDCS-fMRI study. Restor. Neurol. Neurosci. 30 (3), 255–263. http://dx.doi.org/10.3233/RNN-2012-110208.

Bindman, L.J., Lippold, O.C., Redfearn, J.W., 1964. The action of brief polarizing currents on the cerebral cortex of the rat (1) during current flow and (2) in the production of long-lasting after-effects. J. Physiol. 172, 369–382.

Cecere, R., Rees, G., Romei, V., 2015. Individual differences in alpha frequency drive crossmodal illusory perception. Curr. Biol. 25 (2), 231–235. http://dx.doi.org/10.1016/j.cub.2014.11.034.

Creutzfeldt, O.D., Fromm, G.H., Kapp, H., 1962. Influence of transcortical d-c currents on cortical neuronal activity. Exp. Neurol. 5, 436–452.

DeYoe, E.A., Carman, G.J., Bandettini, P., Glickman, S., Wieser, J., Cox, R., Miller, D., Neitz, J., 1996. Mapping striate and extrastriate visual areas in human cerebral cortex. Proc. Natl. Acad. Sci. U. S. A. 93 (1996), 2382–2386.

Fröhlich, F., McCormick, D.A., 2010. Endogenous electric fields may guide neocortical network activity. Neuron 67 (1), 129–143. http://dx.doi.org/10.1016/j.neuron.2010.06.005.

Garcia-Cossio, E., Witkowskia, M., Robinson, S., Cohen, L., Birbaumer, N., Soekadar, S., 2016. Simultaneous transcranial direct current stimulation (tDCS) and whole-head magnetoencephalography (MEG): assessing the impact of tDCS on slow cortical magnetic field. NeuroImage 104, 33–40.

Haegens, S., Nacher, V., Luna, R., Romo, R., Jensen, O., 2011. Alpha-oscillations in the monkey sensorimotor network influence discrimination performance by rhythmical inhibition of neuronal spiking. Proc. Natl. Acad. Sci. U. S. A. 108 (48), 19377–19382. http://dx.doi.org/10.1073/pnas.1117190108.

Helfrich, R.F., Schneider, T.R., Rach, S., Trautmann-Lengsfeld, S.A., Engel, A.K., Herrmann, C.S., 2014. Entrainment of brain oscillations by transcranial alternating current stimulation. Curr. Biol. 24 (3), 333–339. http://dx.doi.org/10.1016/j.cub.2013.12.041.

Herrmann, C., Rach, S., Neuling, T., Strüber, D., 2013. Transcranial alternating current stimulation: a review of the underlying mechanisms and modulation of cognitive processes. Front. Hum. Neurosci. 7, 279. http://dx.doi.org/10.3389/fnhum.2013.00279.

Holland, R., Leff, A.P., Josephs, O., Galea, J.M., Desikan, M., Price, C.J., Rothwell, J.C., Crinion, J., 2011. Speech facilitation by left inferior frontal cortex stimulation. Curr. Biol. 21 (16), 1403–1407. http://dx.doi.org/10.1016/j.cub.2011.07.021.

Kraft, A., Roehmel, J., Olma, M.C., Schmidt, S., Irlbacher, K., Brandt, S.A., 2010. Transcranial direct current stimulation affects visual perception measured by threshold perimetry. Exp. Brain Res. 207 (3-4), 283–290. http://dx.doi.org/10.1007/s00221-010-2453-6.

Logothetis, N., 2008. What we can do and what we cannot do with fMRI. Nature 453 (7197), 869–878. http://dx.doi.org/10.1038/nature06976.

Meinzer, M., Lindenberg, R., Antonenko, D., Flaisch, T., Flöel, A., 2013. Anodal transcranial direct current stimulation temporarily reverses age-associated cognitive decline and functional brain activity changes. J. Neurosci. 33 (30), 12470–12478. http://dx.doi.org/10.1523/JNEUROSCI.5743-12.2013.

Miniussi, C., Brignani, D., Pellicciari, M.C., 2012. Combining transcranial electrical stimulation with electroencephalography: a multimodal approach. Clin. EEG Neurosci. 43 (3), 184–191. http://dx.doi.org/10.1177/1550059412444976.

Nelson, J.T.R., McKinley, A., Golob, E.J., Joel, W.S., Parasuraman, R., 2014. Enhancing vigilance in operators with prefrontal cortex transcranial direct current stimulation (tDCS). NeuroImage 85 (3), 909–917. http://dx.doi.org/10.1016/j.neuroimage.2012.11.061.

Neuling, T., Rach, S., Herrmann, C.S., 2013. Orchestrating neuronal networks: sustained after-effects of transcranial alternating current stimulation depend upon brain states. Front. Hum. Neurosci. 7, 161. http://dx.doi.org/10.3389/fnhum.2013.00161.

Nitsche, M.A., Paulus, W., 2000. Excitability changes induced in the human motor cortex by weak transcranial direct current stimulation. J. Physiol. 527 (Pt 3), 633–639.

Nitsche, M.A., Paulus, W., 2001. Sustained excitability elevations induced by transcranial DC motor cortex stimulation in humans. Neurology 57 (10), 1899–1901.

Nitsche, M.A., Paulus, W., 2011. Transcranial direct current stimulation—update 2011. Restor. Neurol. Neurosci. 29 (6), 463–492. http://dx.doi.org/10.3233/RNN-2011-0618.

Olma, M.C., Kraft, A., Roehmel, J., Irlbacher, K., Brandt, S.A., 2011. Excitability changes in the visual cortex quantified with signal detection analysis. Restor. Neurol. Neurosci. 29 (6), 453–461. http://dx.doi.org/10.3233/RNN-2011-0607.

Pisoni, A., Turi, Z., Raithel, A., Ambrus, G., Alekseichuk, I., Schacht, A., Paulus, W., Antal, A., 2015. Separating recognition processes of declarative memory via anodal tDCS: boosting old item recognition by temporal and new item detection by parietal stimulation. PloS One 10 (3), e0123085. http://dx.doi.org/10.1371/journal.pone.0123085.

Rahman, A., Reato, D., Arlotti, M., Gasca, F., Datta, A., Parra, L.C., Bikson, M., 2013. Cellular effects of acute direct current stimulation: somatic and synaptic terminal effects. J. Physiol. 591, 2563–2578. http://dx.doi.org/10.1113/jphysiol.2012.247171.

Ranieri, F., Podda, M.V., Riccardi, E., Frisullo, G., Dileone, M., Profice, P., Pilato, F., Di Lazzaro, V., Grassi, C., 2012. Modulation of LTP at rat hippocampal CA3–CA1 synapses by direct current stimulation. J. Neurophysiol. 107 (7), 1868–1880. http://dx.doi.org/10.1152/jn.00319.2011.

Reato, D., Rahman, A., Bikson, M., Parra, L., 2010. Low-intensity electrical stimulation affects network dynamics by modulating population rate and spike timing. J. Neurosci. 30 (45), 15067–15079. http://dx.doi.org/10.1523/JNEUROSCI.2059-10.2010.

Ritter, P., Moosmann, M., Villringer, A., 2009. Rolandic alpha and beta EEG rhythms' strengths are inversely related to fMRI-BOLD signal in primary somatosensory and motor cortex. Hum. Brain Mapp. 30, 1168–1187. http://dx.doi.org/10.1002/hbm.20585.

Romei, V., Brodbeck, V., Michel, C., Amedi, A., Pascual-Leone, A., Thut, G., 2008. Spontaneous fluctuations in posterior alpha-band EEG activity reflect variability in excitability of human visual areas. Cereb. Cortex 18 (9), 2010–2018. http://dx.doi.org/10.1093/cercor/bhm229.

Saiote, C., Turi, Z., Paulus, W., Antal, A., 2013. Combining functional magnetic resonance imaging with transcranial electrical stimulation. Front. Hum. Neurosci. 7, 435. http://dx.doi.org/10.3389/fnhum.2013.00435.

Soekadar, S.R., Witkowski, M., Cossio, E.G., Birbaumer, N., Robinson, S.E., Cohen, L.G., 2013. In vivo assessment of human brain oscillations during application of transcranial electric currents. Nat. Commun. 4, 2032. http://dx.doi.org/10.1038/ncomms3032.

Stagg, C.J., 2014. The physiological basis of brain stimulation. Stimul. Brain 145–177 http://dx.doi.org/10.1016/B978-0-12-404704-4.00006-5.

Stagg, C.J., Best, J.G., Stephenson, M.C., O'Shea, J., Wylezinska, M., Kincses, Z.T., Morris, P.G., Matthews, P.M., Johansen-Berg, H., 2009. Polarity-sensitive modulation of cortical neurotransmitters by transcranial stimulation. J. Neurosci. 29 (16), 5202–5206. http://dx.doi.org/10.1523/JNEUROSCI.4432-08.2009.

Turi, Z., Antal, A., Paulus, W., 2012. Functional neuroimaging and transcranial electrical stimulation. Clin. EEG Neurosci. 43 (3), 200–208. http://dx.doi.org/10.1177/1550059412444978.

Wandell, B.A., Dumoulin, S.O., Brewer, A.A., 2007. Visual Field Maps in Human Cortex. Neuron 56, 366–383. http://dx.doi.org/10.1016/j.neuron.2007.10.012.

Witkowski, M., Garcia-Cossio, E., Chander, B.S., Braun, C., Birbaumer, N., Robinson, S.E., Soekadar, S.R., 2016. Mapping entrained brain oscillations during transcranial alternating current stimulation (tACS). NeuroImage 104, 89–98.

Zaehle, T., Rach, S., Herrmann, C.S., 2010. Transcranial alternating current stimulation enhances individual alpha activity in human EEG. PLoS ONE 5 (11), e13766. http://dx.doi.org/10.1371/journal.pone.0013766.